VI CONGRESSO NACIONAL DE ENGENHARIA MECÂNICA
VI NATIONAL CONGRESS OF MECHANICAL ENGINEERING
18 a 21 de agosto de 2010 – Campina Grande – Paraíba - Brasil
August 18 – 21, 2010 – Campina Grande – Paraíba – Brazil

YIELD LOCUS MODELS OF PRESSURIZED PIPES UNDER COMBINED LOADS

Paulo Pedro Kenedi, pkenedi@cefet-rj.br [1]
Lavínia Maria Sanábio Alves Borges, lavinia@mecanica.coppe.ufrj.br [2]
Murilo Augusto Vaz, murilo@peno.coppe.ufrj.br [3]

[1]CEFET/RJ, Department of Mechanical Enginnering, Av. Maracanã, 229 – Maracanã - RJ - CEP 20271-110
[2]UFRJ, Depto. of Mechanical Enginnering, Av. Brigadeiro Trompowsky, s/n – Ilha do Fundão - RJ – CEP 21949-900
[3]UFRJ, Department of Ocean Enginnering, Av. Brigadeiro Trompowsky, s/n – Ilha do Fundão - RJ – CEP 21949-900

Abstract. *Plastic collapse is one of the major causes of failure of pressurized pipes submitted to combined loads. Many models have proposed to estimate the maximum load combination that pressurized pipes can stand. The yield locus pattern is one of the most important attribute of these models. In this work yield locus models are proposed and compared with well established ones.*

Keywords: *yield locus, plastic collapse, pressurized pipes*

1. INTRODUCTION

Limit analysis theory can be used to predict plastic collapse of structures submitted to any combination of loads. This theory distinguishes from incremental plasticity approach by don't following strains evolution, instead determines limit loads where plastic strain keep growing without any further increase of load. In other words, this theory evaluates the limit load that a structure is not longer able to maintain equilibrium with external applied loads. The application of limit analysis theory for structures formed by structural parts, like beams, was extensively studied, as in Hodge (1959). Chattopadhyay (2002), in a more recent investigation, studied the effect of internal pressure on in-plane collapse bending moment of pipes. Robertson (2005) stated that three main types of failure must be considered for the design of pipes: gross plastic deformation, ratchetting and fatigue.

A review of representatives yield locus models for pipes submitted to combined loadings are done, as in Bai and Hauch (1999) where the interaction between pressure P, longitudinal force N and bending moment M in capacity of pipes to resist plastic collapse was analyzed, generating the following yield locus:

$$m = \sqrt{1-\left(1-\alpha^2\right)p^2}\,\cos\left(\frac{\pi}{2}\frac{n-\alpha p}{\sqrt{1-\left(1-\alpha^2\right)p^2}}\right) \tag{01}$$

$$m = \frac{M}{M_0}\ ,\quad n = \frac{N}{N_0}\ \text{ and }\ p = \frac{P}{P_0} \tag{02}$$

Where, m, n and p are respectively the normalized bending moment, the normalized longitudinal load and the normalized internal pressure; M_0, N_0 and P_0 are respectively the bending moment, the longitudinal load and the internal pressure that yields entirely the cross section and α is a correction factor.

The Modified Goodall model, shown at Kim and Oh (2006), using small displacement analysis, proposed a yield locus expression for open-ended elbows under combined loading of internal pressure and in-plane bending:

$$M = 4t\,r_m^2\sigma_y\left(1.04\lambda^{2/3}\right)\left(1-P\frac{r_m}{t\sigma_y}\right)^{1/3} \tag{03}$$

$$P_0 = \frac{t}{r_m}\sigma_y \quad \text{and} \quad M_0 = 4t\,r^2\sigma_y\left(1.04\lambda^{2/3}\right) \tag{04}$$

Substituting (04) in (03) and using (02.a):

$$m = (1-p)^{1/3} \qquad (05)$$

where, t is the wall thickness, r_m is the average radius, σ_y is the limit stress of an elastic-perfectly plastic material, $\lambda = \frac{Rt}{r_m^2}$ is the bend characteristic and R is bend radius.

2. PROPOSED MODEL

At Kenedi et al. (2009) the principal aspects of limit analysis theory, as expressions of equilibrium, kinematics and constitutive relations for straight and curved pipes submitted to concentrated or distributed loads, were covered. The proposition of a yielding function that includes internal pressure (as a dead load) was done as well. The material was considered elastic-perfectly plastic and it was supposed small deformation.

A segment of a pipe submitted to combination of tensile longitudinal load N, positive bending moment M and internal pressure P is show at Fig.1, as well the cross section area and the geometrical variables of a thin-walled pipe:

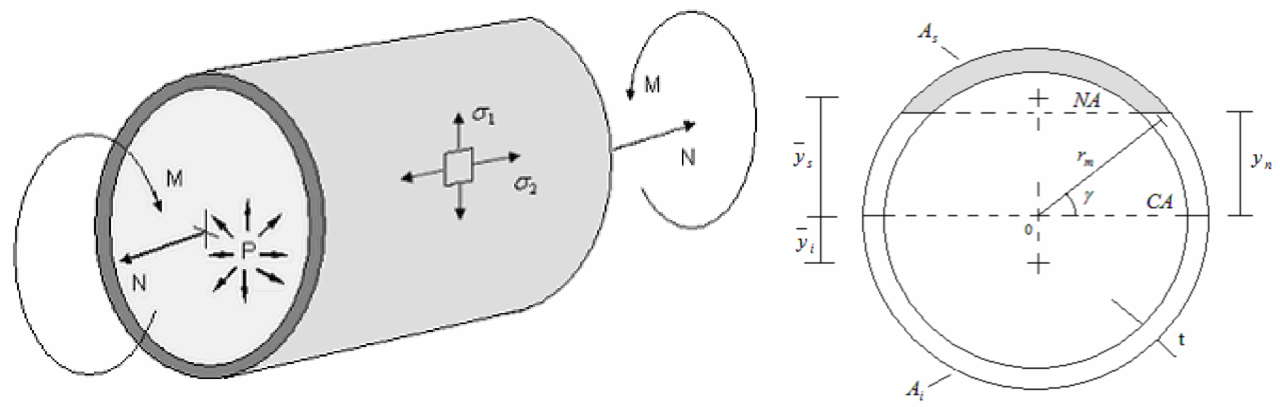

(a) (b)

Figure 1. (a) Segment of a pipe submitted to combination of tensile longitudinal load *N*, positive bending moment *M* and internal pressure *P* and (b) cross section area of a thin-walled pipe for tensile longitudinal load and bending moment.

Where, CA and NA are respectively centroidal and neutral axis, y_n is the distance from CA to NA. The transversal area A is divided in two areas by NA, the superior area A_s (shaded at Fig.1.b) and the inferior area A_i. $\overline{y}_s$ is the distance between centroid of area A (shown with a 0) and the centroid of A_s and $\overline{y}_i$ is the distance between centroid of area A and the centroid of A_i. γ is an angle ranging from $-\frac{\pi}{2}$ to $\frac{\pi}{2}$ rad. The minor area is approximated by $(\pi - 2\gamma)t\,r_m$ and the major area is approximated by $(\pi + 2\gamma)t\,r_m$. At fig. 1.b the minor area is A_s and corresponds to the shaded area. The minor distance is $\left(\frac{2\cos(\gamma)}{\pi + 2\gamma}\right)r_m$ and the major distance is $\left(\frac{2\cos(\gamma)}{\pi - 2\gamma}\right)r_m$.

The application of equilibrium to a pipe segment, submitted to tensile longitudinal force, positive bending moment and internal pressure, shown at Fig.1.a, in combination with the utilization of Mises criterion, were used to obtain the yielding function expressions.

$$\left(\frac{\sigma_1}{\sigma_y}\right)^2 - \frac{\sigma_1}{\sigma_y}\frac{\sigma_2}{\sigma_y} + \left(\frac{\sigma_2}{\sigma_y}\right)^2 = 1 \quad \text{and} \quad \sigma_1 = pP_0\frac{r_m}{t} \qquad (06)$$

$$P_0 = \frac{t}{r_m}\sigma_y \text{ (pipe open-ended) or } P_0 = \frac{2}{\sqrt{3}}\frac{t}{r_m}\sigma_y \text{ (pipe close-ended)} \qquad (07)$$

where, σ_1 and σ_2 are principal stresses.

For open-ended pipes, applying (06.a), (06.b), (02.c) and (07.a), $\frac{\sigma_2}{\sigma_y}$ can be cast as:

$$\frac{\sigma_2}{\sigma_y} = \frac{p}{2} \pm \sqrt{1 - \frac{3}{4}p^2} \text{ or } \frac{\sigma_t}{\sigma_y} = \frac{p}{2} + \sqrt{1 - \frac{3}{4}p^2} \text{ , } \frac{\sigma_c}{\sigma_y} = \frac{p}{2} - \sqrt{1 - \frac{3}{4}p^2} \quad \text{for} \quad p \le 1 \qquad (08)$$

Where σ_t and σ_c are, respectively, the stresses at tensile and compressive areas. For close-ended pipes, applying (06.a), (06.b), (02.c) and (07.b), $\frac{\sigma_2}{\sigma_y}$ can be cast as:

$$\frac{\sigma_2}{\sigma_y} = \frac{p}{\sqrt{3}} \pm \sqrt{1 - p^2} \text{ or } \frac{\sigma_t}{\sigma_y} = \frac{p}{\sqrt{3}} + \sqrt{1 - p^2} \text{ , } \frac{\sigma_c}{\sigma_y} = \frac{p}{\sqrt{3}} - \sqrt{1 - p^2} \quad \text{for} \quad p \le 1 \qquad (09)$$

Figure 2 shows a graphical representation of expressions (08.b), (08.c), (09.b) and (09.c):

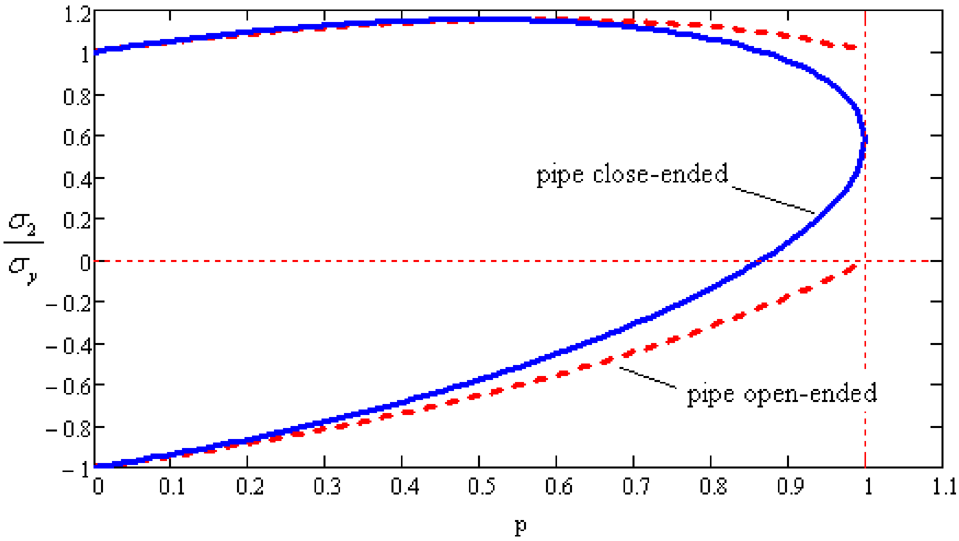

Figure 2. Locus of normalized principal stresses, σ_2/σ_y , as a function of *p*.

Noting that at (6.b) that σ_1 is determined only by internal pressure *P* but not by longitudinal load *N* or by bending moment *M*. Figure 2 shows the maximum values of σ_2/σ_y for various levels of normalized internal pressure, for two extremities patterns: for pipe close-ended and for pipe open-ended. For $p = 0$ both curves has the same performance and they are limited at $p = 1$. As *p* rises the behavior of the two patterns differentiates, with pipe open-ended (dashed curves) reaching higher levels of combinations σ_2/σ_y and *p* than pipe close-ended (continuous curves).

The equilibrium expressions for open-ended pipe can be cast, using (08.b) and (08.c). For the cross section area shown at fig. 1.b ($\sigma_s = \sigma_c$ *and* $\sigma_i = \sigma_t$):

$$\begin{cases} \sigma_s A_s + \sigma_i A_i = N \\ -\sigma_s A_s \bar{y}_s + \sigma_i A_i \bar{y}_i = M \end{cases} \qquad (10)$$

The equilibrium expressions for close-ended pipe can be cast, using (09.b) and (09.c), as:

$$\begin{cases} \sigma_s A_s + \sigma_i A_i = N + \pi r_m^2 P \\ -\sigma_s A_s \bar{y}_s + \sigma_i A_i \bar{y}_i = M \end{cases} \qquad (11)$$

where, $N_0 = 2\pi r_m t \sigma_y$ and, $M_0 = 4 r_m^2 t \sigma_y$ (12)

Solving (10) the yield locus of open-ended pressurized pipe submitted to longitudinal and bending loads are obtained:

$$m = \pm\sqrt{1-\frac{3}{4}p^2}\cos\left[\frac{\pi}{2}\frac{\left(n+\frac{p}{2}\right)}{\sqrt{1-\frac{3}{4}p^2}}\right] \qquad \text{for} \quad n \le 0 \quad (\text{open ended}) \tag{13}$$

$$m = \pm\sqrt{1-\frac{3}{4}p^2}\cos\left[\frac{\pi}{2}\frac{\left(n-\frac{p}{2}\right)}{\sqrt{1-\frac{3}{4}p^2}}\right] \qquad \text{for} \quad n > 0 \quad (\text{open ended}) \tag{14}$$

Similarly, solving (11) the yield locus of close-ended pressurized pipe submitted to longitudinal and bending loads is obtained:

$$m = \pm\sqrt{1-p^2}\cos\left[\frac{\pi}{2}\frac{n}{\sqrt{1-p^2}}\right] \qquad (\text{close-ended}) \tag{15}$$

For a particular case of null longitudinal load, $n = 0$, expressions (13) and (15), can be rewritten, respectively, to:

$$m = \pm\sqrt{1-\frac{3}{4}p^2}\cos\left[\frac{\pi}{2}\frac{\frac{p}{2}}{\sqrt{1-\frac{3}{4}p^2}}\right] \qquad (\text{open-ended}) \tag{16}$$

$$m = \pm\sqrt{1-p^2} \qquad (\text{close-ended}) \tag{17}$$

Figure 3 shows a graphical representation of expressions (16) and (17), for $0 \le p \le 1$ and $0 \le m \le 1$:

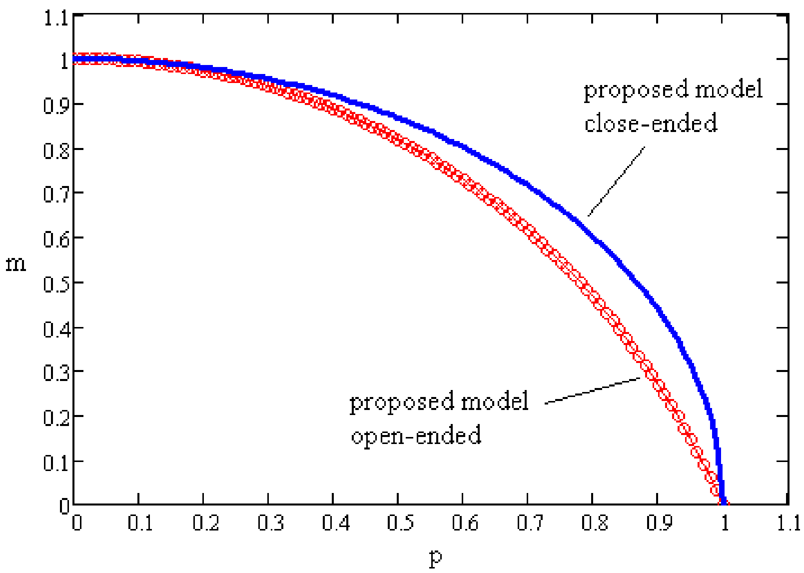

Figure 3. Comparative graphic *p* versus *m* of yield locus (*n* = 0) for the proposed model with different endings.

Figure 3 shows the yield locus for the proposed model, for $n = 0$, with different endings. For $p = 0$ and for $p = 1$ both curves have the same performance. For $0 < p < 1$ the close-ended (blue curve) permits higher combinations of m and p than open-ended (red curve).

For a particular case of null internal pressure, $p = 0$, the expressions (13), (14) and (15) can be cast as:

$$m = \pm\cos\left[\frac{\pi}{2}n\right] \tag{18}$$

Figure 4 shows the limiting yielding surfaces, respectively for open-ended and close-ended pipes, calculated from the application of expressions (13), (14) and (15), submitted to a combination of longitudinal load *N*, bending moment *M* and internal pressure *P*:

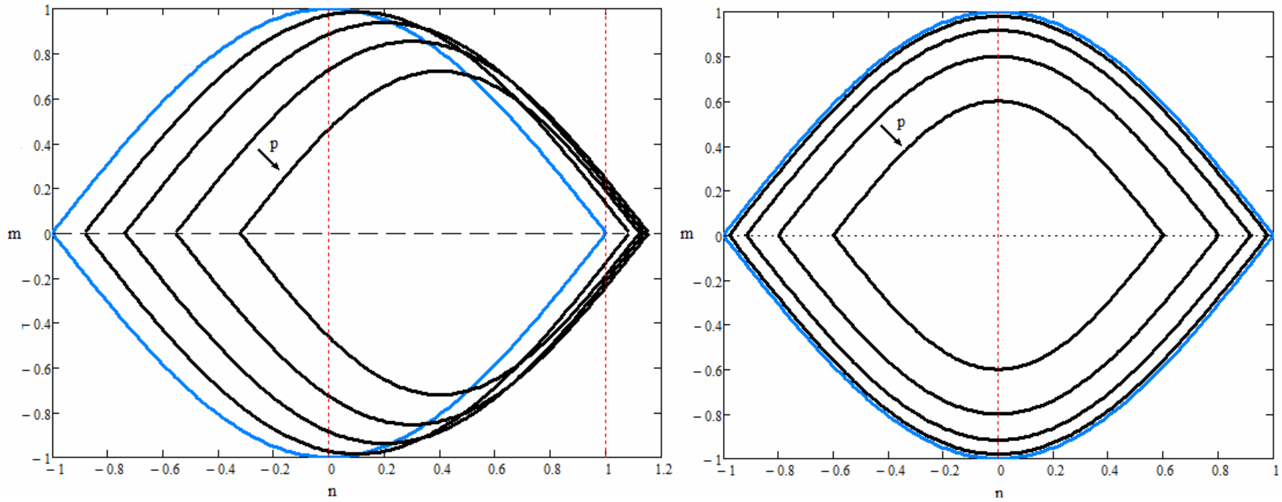

(a) (b)

Figure 4. Limiting yielding surfaces for: (a) open-ended and (b) close-ended pipes.

Figure 4 presents two graphics for values of *n* versus *m*, for normalized pressures $0 \leq p \leq 0.8$, with increments of 0.2*p*. Note that the arrows shows direction that *p* increases. At Figs. 4.a and 4.b, for *p* = 0 the limiting yielding surfaces are the large ones (blue curves). As *p* increases the limiting yielding surfaces become smaller. For open-ended pipes the limiting yielding surfaces moves to the rigth side of the graph and become smaller as *p* increses, while for close-ended pipes the limiting yielding surfaces maintain concentric and also become smaller as *p* increses.

3. COMPARISON

The Modified Goodall model for combined loading of internal pressure and in-plane bending of pipes, expression (05), is compared with expression (16) of the open-ended proposed model, with results shown graphically at figure 5:

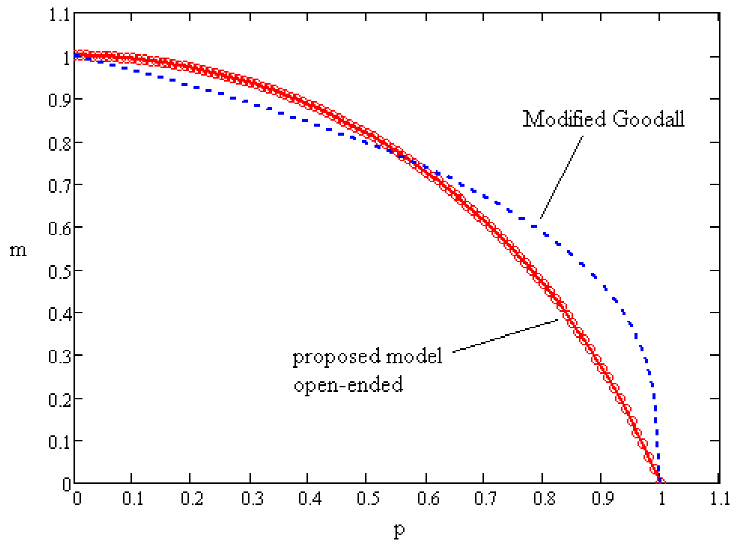

Figure 5. Comparative graphic *p* versus *m* of yield locus of analyzed models.

Figure 5 shows, for any λ and *n* = 0, the performance of the models of yield locus for pipes submitted to combined loading of internal pressure and in-plane bending. Note that M_0 definitions for the Modified Goodall model, expression (04.b), and for the open-ended presented model, expression (12.b), aren't the same. The proposed model presented good agreement with the Modified Goodall model used as reference.

4. CONCLUSIONS

A model to determine the yield locus of pressurized pipes submitted to combined loadings of longitudinal force, bending moment and internal pressure was presented. The expressions for all three loadings as well as with especial cases of no internal pressure or no longitudinal force were analyzed. The behavior differences between open-ended and close-ended pipe terminations were also analyzed. The proposed model with open-ended and no longitudinal force was compared with the Modified Goodall model with good agreement.

5. REFERENCES

Bai, Y., 2001, "Pipelines and Risers", Volume 3, Elsevier Ocean Engineering Book Series.

Bai, Y., Damsleth, Per A., S., Gustafsson, C. and Nystrom, Per R., 1999, "Deepwater pipeline installation with plastic strain", Proceedings of the 18th International Conference on Offshore Mechanics and Artic Engineering – OMAE 1999, Newfoundland, Canada.

Bai, Y., Igland, R.T. and Moan, T., 1997, "Tube Collapse Under Combined External Pressure, Tension and Bending", Marine Structures, Vol. 10, pp. 389-410.

Borges, L.A., Zouain, N. and Huespe, A.E., 1996, "A nonlinear optimization procedure for limit analysis", Eur. J. Mech. A/Solids, Vol. 15(3), pp.487-512.

Borges, L.M.S.A., 1991, "Formulação e Solução para Análise Limite com Superfícies de Escoamento Não Linear", Tese de Doutorado, PUC-Rio, Rio de Janeiro, Brasil.

Chattopadhyay, J., 2002, "The effect of internal pressure on in-plane collapse moment of elbows", Nuclear Engineering and Design, Vol. 212, pp. 133-144.

Hauch, S. and Bai, Y., 1999, "Bending Moment Capacity of Pipes", Proceedings of the 18th International Conference on Offshore Mechanics and Artic Engineering – OMAE 1999, Newfoundland, Canada.

Hodge, P.G., 1959, "Plastic Analysis of Structures", Mc Graw Hill.

Lubliner, J., 1990, "Plasticity Theory", McMillan Publishing Company.

Kenedi, P.P., Borges, L.M.S.A. and Vaz, M.A., 2009, "Plastic Collapse of Pressurized Pipes", 30º CILAMCE, Búzios, Rio de Janeiro.

Kenedi, P.P., 2008a, "Análise Limite em Dutos", Tese de Doutorado, COPPE-UFRJ, Rio de Janeiro, Brasil.

Kenedi, P.P., Borges, L.M.S.A. and Vaz, M.A., 2008b, "The Interection Between Pressure and Bending Loadings in Pipe Collapse", V Congresso Nacional de Engenharia Mecânica – CONEM 2008, Salvador, Bahia.

Kim, Y. and Oh, C., 2006, "Closed-form plastic collapse loads of pipe bends under combined pressure and in-plane bending", Engineering Fracture Mechanics, Vol. 73, pp. 1437-1454.

Offshore Standard, 2000, "DNV-OS-F101 - Submarine Pipeline Systems", Det Norske Veritas.

Robertson, A., Li, H. and Mackenzie, D., 2005, "Plastic collapse of pipe bends under combined internal pressure and in-plane bending", Pressure Vessels and Piping, Vol. 82, pp. 407-416.

Sanabio, L.M.M., 1984, "Análise limite em pórticos via otimização", Dissertação de Mestrado, PUC-Rio, Brasil.

6. RESPONSIBILITY NOTICE

The authors are the only responsible for the printed material included in this paper.